Journal of ELECTRONIC MATERIALS, Vol. 50, No. 4, 2021
https://doi.org/10.1007/s11664-020-08430-1

ASIAN CONSORTIUM ACCMS–INTERNATIONAL CONFERENCE ICMG 2020

Insights into the Ground-State Charge Transfer in Conjugated Polymer Donor–Acceptor Complexes

SHEIK HASEENA[1] and MAHESH KUMAR RAVVA[1,2]

1.—Department of Chemistry, SRM University-AP, Amaravati, Andhra Pradesh 522508, India.
2.—e-mail: mahesh.r@srmap.edu.in

Van der Waals type forces are generally responsible for the stability of conjugated polymer–acceptor complexes, and no charge transfer is observed in the ground state. Electron transfer generally occurs from donor materials to acceptor materials via photoinduced electron transfer. Here, we report a partial ground-state charge transfer in the all-polymer donor–acceptor interface using density functional theory-based methods such as long-range corrected ωB97XD and hybrid meta exchange–correlation M06 functionals. These methods are also used to evaluate the geometrical and electronic properties of conjugated polymers in the neutral and charged states.

Key words: Donor–acceptor complexes, charge-transfer interactions, conjugated polymers, density functional theory

INTRODUCTION

Understanding the nature of the interaction between the blends of conjugated polymers is of growing interest for organic solar cell and light-emitting device applications.[1–3] The active layer of all-polymer organic solar cells contains donor–acceptor blends consisting of two different conjugated polymers. Several studies have demonstrated that these blends can be used for effective photocurrent generation and efficient light emission.[4,5] For application to organic solar cells and photodetectors, the interface between the conjugated donor polymers and acceptor polymers facilitates the dissociation of excitons that are generated in either material. Excitons dissociate into separate charges and reach different electrodes, and so deliver a photocurrent.[6] For application to polymer light-emitting devices, donor and acceptor conjugated polymers are responsible for transporting electrically injected charges toward the interface, where charge association and radiative recombination may occur. All these electronic processes critically depend on energy level alignment between donor and acceptor materials, the morphology of the active layer, and charge transport properties.[7]

Energy level alignment between donor and acceptor materials, the morphology of the active layer, and charge transport are the key parameters that dictate the efficiency of the device. Charge transport properties and morphology of blends of conjugated polymers substantially depend on the intermolecular interactions between donor and acceptor polymers. Several studies have been devoted to understanding the nature of the interaction between conjugated polymers and various acceptor materials.[1,2,8,9] It is found that in the case of strong small-molecule acceptors such as tetracyanoquinodimethane (TCNQ) and 2,3,5,6-tetrafluoro-7,7,8,8-tetracyanoquinodimethane (F4-TCNQ), some degree of ground-state charge transfer is observed, while in the case of fullerene-based acceptor materials, no charge transfer from donor to the acceptor in the ground state is observed, and van der Waals interactions are responsible for the stability of donor–acceptor complexes.[1,2] However, the nature of intermolecular interactions between conjugated donor and conjugated acceptor polymer systems is not fully understood.

(Received June 14, 2020; accepted August 18, 2020;

Several strategies have been introduced to increase the charge transport properties in organic materials.[10–12] One such strategy is the doping of heterogeneous molecules or polyelectrolytes. The major challenge associated with these dopants is they become redundant in the active layer once the electronic doping process is completed. These dopant materials sometimes even show a negative effect on charge transport properties during the device operation. Another issue with the polymer-dopant systems is the thermal stability. At higher temperatures, these polymer-dopant systems can undergo rapid sublimation, leading to degradation of the electronic properties. Recently, Fabanio and co-workers demonstrated ground-state electron transfer in all-polymer heterojunctions without heterogenous doping.[13] Spontaneous charge transfer between the donor polymer and acceptor was demonstrated by combining the low-ionization-energy polymers with high-electron-affinity polymer counterparts. Here in this study, we seek to gain a better understanding of the electronic structure of ground-state charge-transfer complexes made up of two different conducting polymers. We present a systematic theoretical study on the interface between oligomer complexes, which are stabilized by π-π interactions. We report the geometrical and electronic properties of these complexes along with the amount of charge transferred from the donor oligomer to acceptor oligomer in the ground state.

COMPUTATIONAL METHODOLOGY

Choosing an appropriate density functional method to calculate the geometrical and electronic properties of weakly bound complexes and estimate the interaction energy is always challenging. In this study, we have considered two different functionals: a long-range and dispersion-corrected ωB97XD functional and a hybrid meta exchange–correlation M06 functional. It has been shown that these functionals show better performance than the B3LYP functional.[14–17] Geometry optimizations of neutral and charged isolated oligomer chains and polymer complexes were achieved using M06 and ωB97XD functionals in conjunction with a 6–31 g(d) basis set. In order to understand the nature of the interaction between the chains, single-point vertical scanning calculations were performed by varying the distance between two oligomer backbones. Furthermore, the charge-transfer calculations were carried out using natural population analysis (NPA) with the M06/6-31 g(d,p) and ωB97XD/6-31 g(d,p) methods using the optimized geometries. All calculations were performed using the Gaussian 16 package.[18]

Models Considered in the Study

Density functional theory (DFT) calculations are a useful tool to predict and assess the geometrical, electronic, and charge-transfer properties of conjugated polymers.[19,20] In order to understand the ground-state charge transfer between donor and acceptor polymers, four conjugated donor and three ladder-type acceptor polymers are considered in this study. The donor polymers, poly thiophene (PT) and its derivative, poly(2,5-bis(3-alkylthiophen-2-yl)thieno[3,2-b]-thiophene) (BTTT), indacenodithiophene-dithieno[3′,2′:3,4;2′,3′:5,6]benzo[1,2-c]-[1,2,5] thiadiazole (IDTDTBT), indacenodithiophene-[1,2,5] thiadiazolo[3,4-b]dithieno[3,2-f:2′,3′-h]quinoxaline (IDTDTBPT), are chosen as donor polymers.[21] Three acceptor ladder-type polymers, benzimidazobenzophenanthroline (BBL) and its fluorinated (BBL-F), and cyano (BBL-CN)-substituted polymers are considered as acceptor materials.[22]

Thiophene oligomer with 12 thiophene units (TPD), four repeating units of bithiophene and thienothiophene (BTTT), trimeric units (for copolymer systems, IDTDTBT and IDTDTPBT systems), and tetrameric repeating units (BBL, BBL-F, and BBL-CN) in acceptor polymers are considered as model systems. Generally, these conjugated polymers are appended with the long alkyl side chains to enhance the solubility. In order to reduce the computational cost, the long alkyl side chains were replaced with hydrogen atoms.

RESULTS AND DISCUSSION

As a first step, we would like to gain more insights into the geometrical and electronic properties of neutral and charged isolated oligomer chains. The electronic properties of conjugated polymers strongly depend on the various geometrical properties such as bond lengths across the backbone, dihedral angles between adjacent electron-rich and electron-poor units, and relative coplanarity of electron-rich and electron-poor copolymer segments. The coplanar backbone not only facilitates the effective charge delocalization across the backbone but also enhances the intermolecular coupling with other the polymer chains. The optimized geometries of donor and acceptor oligomers considered in this study are depicted in Figs. 1 and 2. In the cases of donor oligomers considered in this study, in the neutral state, the PT and PBTTT oligomers have shown twists (around 12°) in the dihedral angles between the units and hence could exhibit lower conjugation lengths. Both IDT-based donor oligomers (IDTDTBT and IDTDTBPT) have a coplanar backbone, and the high aromatic character of electron-rich units results in lower ionization energy in these polymers. BBL is a unique polymer in which one imidazole ring is fused between naphthalene and benzene units. All acceptor conjugated oligomers, namely BBL, BBL-F, and BBL-CN, have a very rigid backbone.

The calculated single-electron highest occupied molecular orbitals (HOMO) of donor oligomers and lowest unoccupied molecular orbitals (LUMO) of acceptors are shown in Fig. 3 along with HOMO and

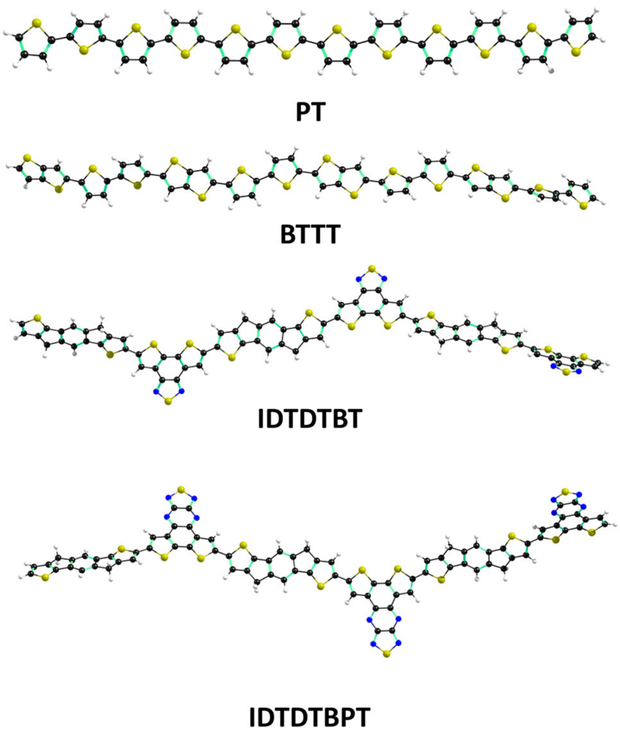

Fig. 1. Optimized geometries of neutral donor oligomers as determined at the ωB97XD/6-31G(d) level of theory.

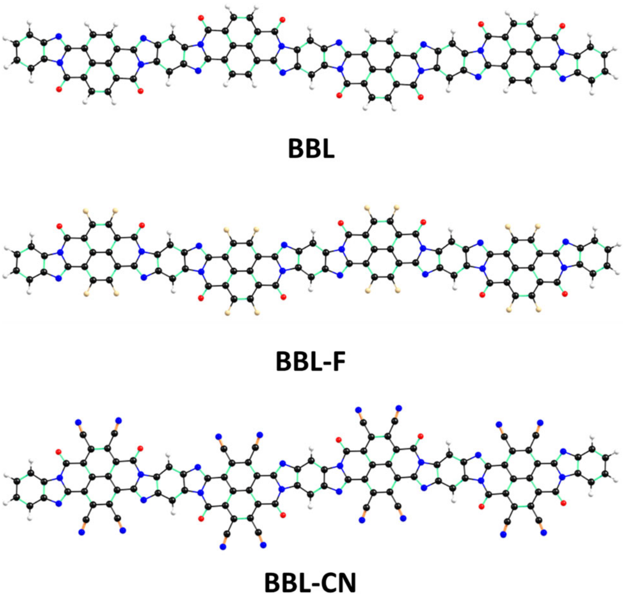

Fig. 2. Optimized geometries of neutral donor oligomers as determined at the ωB97XD/6-31G(d) level of theory.

LUMO energy vales as obtained with the M06/6-31d(d) method. It can be noted from these wave functions that in the case of donor oligomers, the electron density is delocalized along the backbone, whereas in the case of acceptor oligomers, the electron density is primarily localized on the naphthalene units. In the case of donor oligomers, we have considered different combinations of electron-rich and electron-poor units. However, we have noted similar HOMO values for all donor oligomers which is the range of –5.0 eV. In the case of acceptor oligomers, unsubstituted BBL oligomer has a LUMO energy value around −2.3 eV. Upon substitution of electron-withdrawing functional groups such as –F and –CN groups on the periphery of the BBL backbone, the LUMO value is further stabilized. Especially in the case of BBL-CN oligomer, the LUMO value shifted to −3.71 eV due to strong inductive effect of –CN groups. The ground-state charge transfer strongly depends on the energy level matching between the HOMO of the donor and the LUMO of the acceptor. One can observe from these energy levels that these oligomers can exhibit ground-state charge transfer from donor oligomer to acceptor oligomer as the energy difference between HOMO and LUMO levels are less.

GEOMETRICAL AND ELECTRONIC PROPERTIES UPON DOPING

The electronic and optical properties of conducting polymers strongly depend on the degree of π-electron delocalization along the backbone and the formation of polarons (singly charged quasiparticles).[23] The polarons are localized on the backbone of the conjugated polymer due to electron–phonon coupling. When a donor polymer with low ionization potential interacts with an acceptor polymer with high electron affinity, electrons are transferred from the donor to acceptor, leading to the formation of a hole polaron on the donor oligomer and an electron polaron on the acceptor oligomer, and such polarons play a crucial role in the charge transport properties.

In order to understand how the charge doping process impacts the geometrical and electronic properties of oligomers considered in this study, we first study oxidized (doping a positive charge) donor oligomers and reduced (doping a negative charge) acceptor oligomers. An extra electron added to the acceptor oligomer results in a doublet state wave function with one unpaired electron of the spin S = 1/2. Similarly, removing an electron (doping of hole) from the donor oligomers results in a doublet state wave function with one unpaired electron of the spin S = 1/2. The calculated hole polaron wave functions on donor oligomers and electron polarons on acceptor oligomers are shown in Fig. 4.

It can be seen from Fig. 4 that the hole polaron on the thiophene-based oligomer is delocalized over six thiophene rings. Also, upon hole doping, the backbone becomes completely coplanar. Similar results also observed in BTTT-based oligomer. In the cases of IDT-based oligomers, the hole polaron is distributed over two repeating units. Unlike in the case of hole polarons, the electron polarons are localized on naphthalene units. As we discussed earlier, BBL and its derivative oligomers have both benzene and

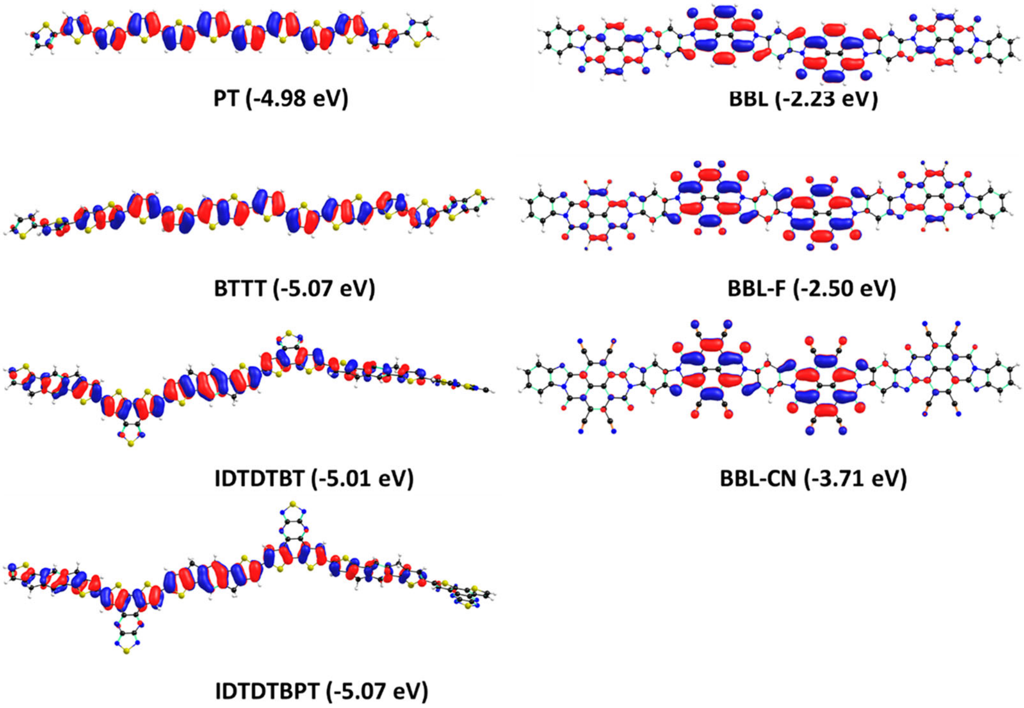

Fig. 3. Pictorial representation of single-electron HOMOs of donor oligomers (left) and LUMOs of acceptor oligomers as determined at the M06/6-31G(d) level of theory.

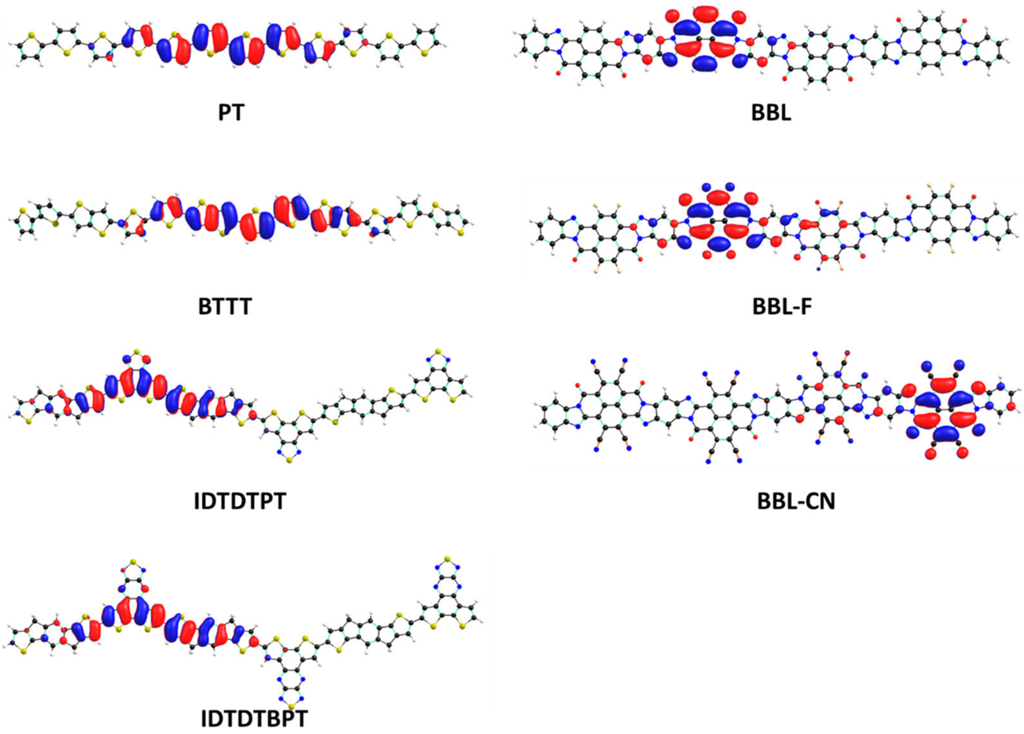

Fig. 4. Pictorial representation of the hole polaron (left) in donor oligomers and electron polaron (right) in acceptor oligomers as determined at the M06/6-31G(d) level of theory.

naphthalene units in the backbone. As evidenced from Fig. 4, the electron polaron in BBL, BBL-F, and BBL-CN oligomers is mostly localized on naphthalene units. The calculated electron polaron distribution in the case of the BBL oligomer is in good agreement with the previous results.[24] The analysis of nuclear displacements also provides more insights into the polaron's localized nature for donor and acceptor oligomers. Figures 5 and 6 report the bond length differences (BLDs) for the hole and electron polarons in donor and acceptor oligomers, respectively. Here, BLDs are calculated as the difference in the bond length of each bond in charged and neutral states. Upon addition/removal of an electron, some bonds undergo contraction and some bonds undergo expansion compared to neutral-state bond lengths. Thus, BLDs demonstrate how geometrical parameters vary when an electron is added/removed. BLD graphs for each donor and acceptor oligomer clearly reveal the localized nature of polarons. In the case of thiophene-based donor oligomers such as PT and BTTT, large changes in bond lengths (from −0.03 to 0.05 Å) are observed, whereas as in the case IDT-based oligomer, the BLDs are slightly less. When a polaron is delocalized on a larger number of units, BLDs will generally be smaller (the length of the polaron in PT and BTTT is around 21 Å, whereas in the case of IDT-based oligomers, the same value is around 30 Å). We also note that, compared to donor oligomers, small BLDs are observed in acceptor oligomer cases.

We have also calculated reorganization energies related to hole and electron transport of donor and acceptor oligomers, respectively employing M06 and ωB97XD methods. The calculated hole and electron reorganization energies for the considered donor and acceptor oligomers are listed in Table I. Even though the magnitude of calculated hole and electron reorganization energies are quite different for M06 and ωB97XD functionals, they are in a similar trend. A significant difference between reorganization values is attributed to the fundamental nature of density functionals (M06 and ωB97XD) consider here. The M06 functional is a hybrid meta-GGA functional, and it has a fixed fraction of the HF exchange (27% HF) and it suffers from self-interaction energy errors. This leads to the spurious delocalization of charge distribution and overestimation of conjugation. Thus, lower reorganization values are obtained compared to the ωB97XD method. The long-range correction in the ωB97XD functional predicts the proper description of wave function delocalization; hence, higher reorganization energies are observed compared to the M06 functional. In the case of the BBL oligomer, the calculated electron reorganization energy values are in good agreement with the previous report.[25] Small reorganization energies, coplanar backbones, and large polaron distribution across the backbone

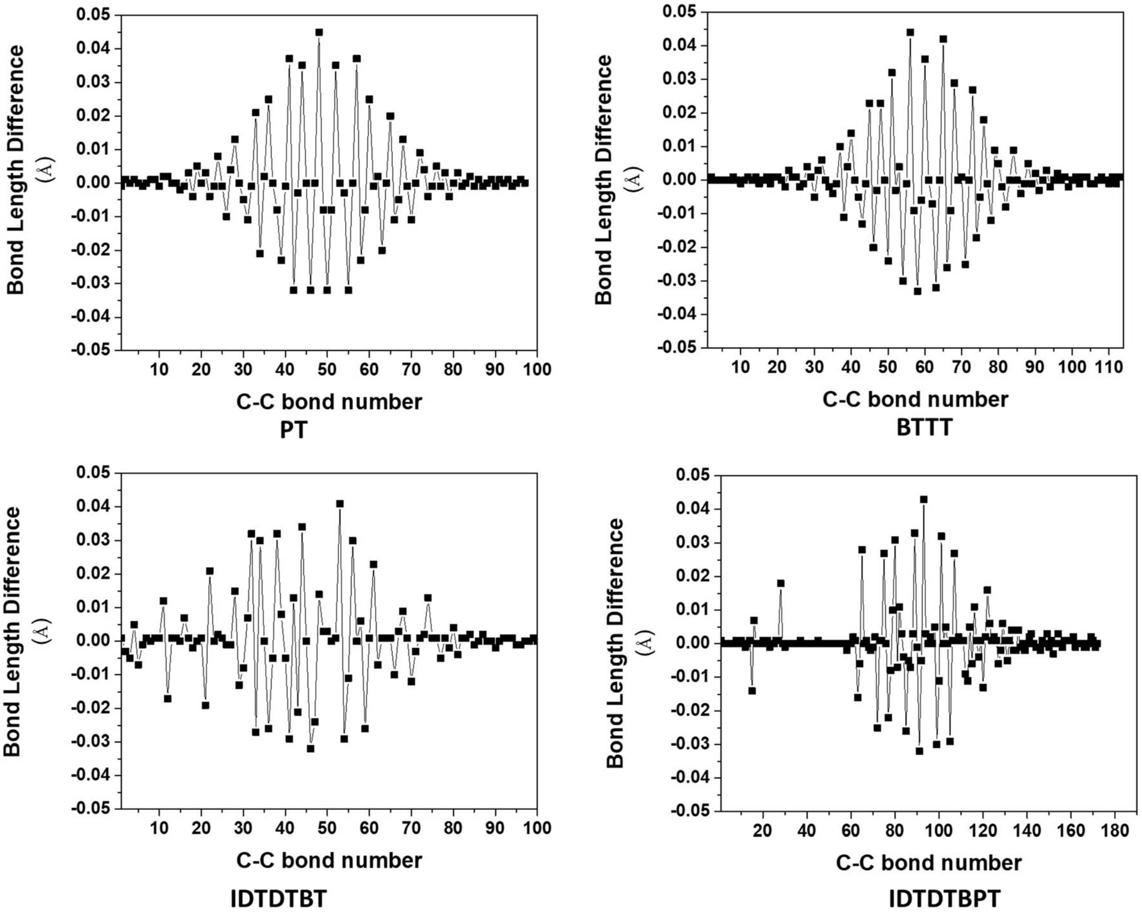

Fig. 5. BLDs of different donor oligomers considered in this study as determined at the M06/6-31G(d) level of theory.

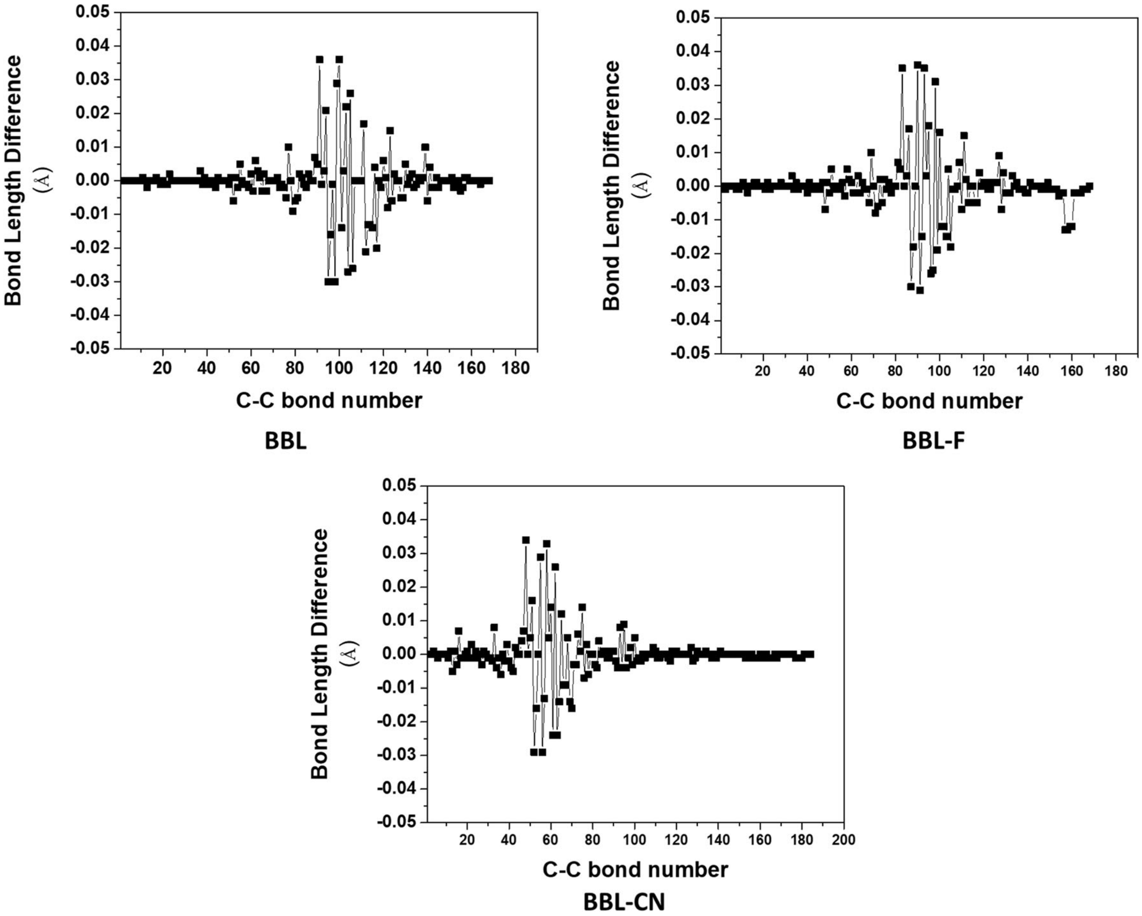

Fig. 6. BLDs of different acceptor oligomers considered in this study as determined at the M06/6-31G(d) level of theory.

Table I. Calculated hole reorganization energies (for donor oligomers) and electron reorganization energies (for acceptor oligomers) at M06/6-31 g(d) and ωB97XD/6-31 g(d) levels of theory

	M06/6-31 g(d)		ωB97XD/6-31 g(d)	
	Hole	Electron	Hole	Electron
PT	205	–	674	–
BTTT	181	–	658	–
IDTDTBT	126	–	519	–
IDTDTBPT	118	–	519	–
BBL	–	87	–	310
BBL-F	–	100	–	320
BBL-CN	–	80	–	304

All values are given in meV.

clearly suggest that the oligomers consider in this study show good charge transport.

GROUND-STATE CHARGE TRANSFER

In donor–acceptor complexes, the ground-state wave function can be considered as a linear combination of the neutral donor and acceptor molecules plus charge-transfer state wave function.[26] In the framework of a single determinantal description of the ground-state wave function, charge transfer can be considered as electron transfer from the HOMO of the donor to the LUMO of the acceptor. Hence, the energy difference between these orbitals and electronic coupling are crucial parameters to calculate the amount of charge transferred.

As mentioned in the methodology section, single-point energy vertical scanning calculations were performed by varying the distance between two oligomer backbones. During the scanning, the molecular planes of both oligomers are kept parallel to one another in the cofacial geometry. The intermolecular distances are varied from 3 Å to 5 Å. We found that all complexes demonstrated energy minima around 3.5 Å. The calculated HOMOs of donor oligomers, LUMOs of acceptor oligomers, HOMO–LUMO gaps (HLG) of donor–acceptor complexes, along with the charge transfer from the donor to acceptor calculated using natural population analysis, are given in Table II.

The computed HOMOs of donor chains in the presence of BBL oligomers are in the range of − 5.0 eV (based on M06 values). The same values in the presence of BBL-F and BBL-CN are in the

Table II. Computed HOMO (donor)–LUMO (acceptor) values, HOMO–LUMO gaps (HLG), and calculated charge transfer (CT) for various donor–acceptor oligomer complexes using M06/6-31 g(d,p) and ωB97XD/6-31 g(d,p) methods. HOMO, LUMO, and HLG are given in eV

	ωB97XD/6-31 g(d,p)				M06/6-31 g(d,p)			
Complexes	**HOMO**	**LUMO**	**HLG**	**CT**	**HOMO**	**LUMO**	**HLG**	**CT**
PT-BBL	− 6.35	− 2.13	4.22	0.01	− 4.99	− 3.49	1.50	0.02
BTTT-BBL	− 6.39	− 2.12	4.27	0.03	− 5.03	− 3.46	1.57	0.04
IDTDTBT-BBL	− 6.44	− 2.17	4.27	0.04	− 5.07	− 3.51	1.55	0.05
IDTDTBPT-BBL	− 6.48	− 2.21	4.27	0.04	− 5.12	− 3.56	1.57	0.06
PT-BBL-F	− 6.57	− 2.25	4.32	0.02	− 5.20	− 3.63	1.57	0.02
BTTT-BBL-F	− 6.54	− 2.23	4.31	0.02	− 5.18	− 3.61	1.57	0.03
IDTDTBT-BBL-F	− 6.58	− 2.30	4.28	0.04	− 5.21	− 3.67	1.54	0.07
IDTDTBPT-BBL-F	− 6.63	− 2.34	4.29	0.03	− 5.27	− 3.72	1.55	0.06
PT-BBL-CN	− 7.00	− 3.50	3.49	0.02	− 5.63	− 4.80	0.82	0.05
BTTT-BBL-CN	− 6.96	− 3.48	3.48	0.04	− 5.60	− 4.78	0.82	0.09
IDTDTBT-BBL-CN	− 6.92	− 3.52	3.40	0.08	− 5.58	− 4.79	0.79	0.22
IDTDTBPT-BBL-CN	− 6.95	− 3.55	3.40	0.08	− 5.60	− 4.81	0.79	0.22

The CT value is given in au.

ranges of − 5.1 eV and − 5.6 eV, respectively. Similarly, LUMOs of acceptor chains are also stabilized in the presence of donor chains. This clearly shows that both the donor and acceptor oligomer chains are strongly polarizing each other. We believe the shift in the energy levels is primarily due to polarization only as these chain interacts through π-π interactions. Charge transfer may not influence the position of energy levels. The LUMO energy values of PT-BBL-CN and IDTDTBPT-BBL-CN are almost the same (−4.80 eV and − 4.81 eV) even though there is a partial charge transfer in the latter case. The charge-transfer value strongly depends on the energy difference between HOMO and LUMO orbitals (HLG). As the HLG values decrease, higher charge transfer is observed. It can be seen from Table II that a partial charge transfer (0.22 au) is observed only in the cases of IDTDTBT-BBL-CN and IDTDTBPT-BBL-CN complexes.

In the previous section, we showed how geometries of donor and acceptor oligomers vary in the limit of full transfer of electrons (by removing and adding an electron). However, the single-point energy calculations of donor–acceptor complexes show only a partial charge transfer (around 0.22 |e|) from the donor oligomer to acceptor oligomer. In order to quantify the amount of charge transfer in these donor–acceptor complexes, geometry optimizations were carried out only in the cases of BBL-CN acceptor oligomer interaction with different donor oligomers. The optimized geometries of these complexes are depicted in Fig. 7, along with the CT values. It can be seen from the figure that a partial charge is transferred from the donor to acceptor, and these values are much higher in IDTDTBPT oligomer (0.38 |e|). The average intermolecular distance between chains is around 3.5 Å. All these calculations clearly evidence the partial ground-state charge transfer in these systems.

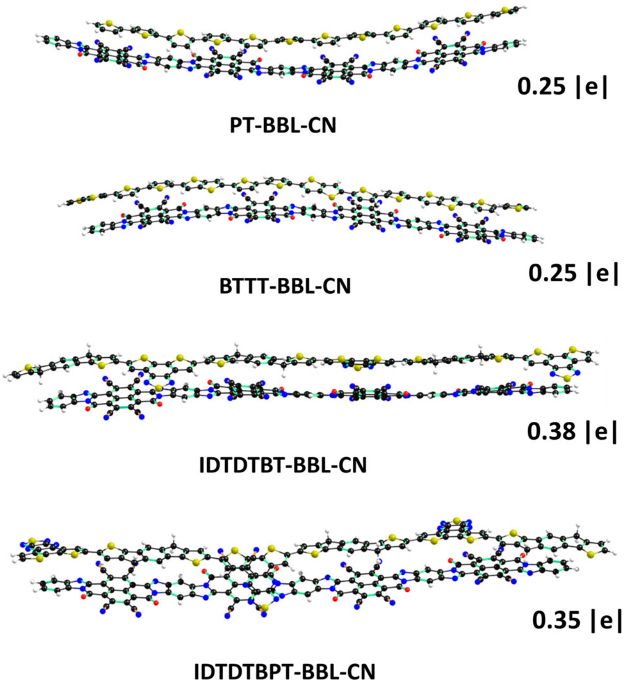

Fig. 7. Optimized geometries of donor–BBL–CN complexes obtained at M06/6-31 g(d) level of theory.

CONCLUSIONS

Density functional theory-based calculations have been carried out on various donor–acceptor complexes to understand their geometrical and electronic properties. Furthermore, natural population analysis has been carried out on these complexes to evaluate their ground-state charge-transfer properties. The long-range corrected ωB97XD and hybrid meta exchange–correlation M06 functionals are used to predict the charge distribution, delocalization of polaron wave function, and structural deformations in the neutral and charge states. The calculated low reorganization energy values and small structural deformations show that these polymers can exhibit good charge transport properties. In donor–acceptor oligomer complexes, the intermolecular interactions at the interface between donor and acceptor oligomers induced the polarization energies, which led to the stabilization of HOMO and LUMO energies of conjugated oligomers. Generally, in the case of donor–acceptor complexes, the electron transfer from the donor to the acceptor occurs via photoinduced electron transfer. From our calculations, a partial charge transfer from the donor to acceptor has been observed, especially in the case of cyano-substituted acceptor oligomers in the ground state. We believe that these results may provide some critical clues when designing new organic materials for solar cell, thermoelectric, wearable electronic, and light-emitting diode applications.

ACKNOWLEDGMENTS

We thank the Department of Science and Technology (DST), New Delhi, India, for support of this research under the DST-INSPIRE scheme (DST/INSPIRE/04/2017/001393). We would like to thank the SRM Supercomputer Center, SRM Institute of Science and Technology for providing the computational facility.

CONFLICT OF INTEREST

The authors declare that they have no conflict of interest.

REFERENCES

1. M.K. Ravva, T. Wang, and J.-L. Brédas, *Chem. Mater.* 28, 8181 (2016).
2. S. Sweetnam, K. Vandewal, E. Cho, C. Risko, V. Coropceanu, A. Salleo, J.-L. Brédas, and M.D. McGehee, *Chem. Mater.* 28, 1446 (2016).
3. I. Angunawela, M.M. Nahid, M. Ghasemi, A. Amassian, H. Ade, and A. Gadisa, *ACS. App. Mater. Interfaces* 12, 26239 (2020).
4. R.H. Friend, R.W. Gymer, A.B. Holmes, J.H. Burroughes, R.N. Marks, C. Taliani, D.D.C. Bradley, D.A.D. Santos, J.L. Brédas, M. Lögdlund, and W.R. Salaneck, *Nature* 397, 121 (1999).
5. V. Coropceanu, J. Cornil, D.A. da Silva Filho, Y. Olivier, R. Silbey, and J.-L. Brédas, *Chem. Rev.* 107, 926 (2007).
6. J.-L. Brédas, J.E. Norton, J. Cornil, and V. Coropceanu, *Acc. Chem. Res.* 42, 1691 (2009).
7. S.M. Ryno, M.K. Ravva, X. Chen, H. Li, and J. Brédas, *Adv. Energy Mater.* 7, 1601370 (2017).
8. J.-L. Brédas, D. Beljonne, V. Coropceanu, and J. Cornil, *Chem. Rev.* 104, 4971 (2004).
9. G. Duva, P. Beyer, R. Scholz, V. Belova, A. Opitz, A. Hinderhofer, A. Gerlach, and F. Schreiber, *Phys. Chem. Chem. Phys.* 21, 17190 (2019).
10. B. Lüssem, C.-M. Keum, D. Kasemann, B. Naab, Z. Bao, and K. Leo, *Chem. Rev.* 116, 13714 (2016).
11. Y. Xu, H. Sun, A. Liu, H.-H. Zhu, W. Li, Y.-F. Lin, and Y.-Y. Noh, *Adv. Mater.* 30, 1801830 (2018).
12. J. H. Oh, A.-R. Han, H. Yu, E. K. Lee, and M. J. Jang, in edited by Z. Bao, I. McCulloch, R. Shinar, and I. Kymissis (San Diego, California, United States, 2013), p. 883112.
13. K. Xu, H. Sun, T.-P. Ruoko, G. Wang, R. Kroon, N.B. Kolhe, Y. Puttisong, X. Liu, D. Fazzi, K. Shibata, C.-Y. Yang, N. Sun, G. Persson, A.B. Yankovich, E. Olsson, H. Yoshida, W.M. Chen, M. Fahlman, M. Kemerink, S.A. Jenekhe, C. Müller, M. Berggren, and S. Fabiano, *Nat. Mater.* 19, 738 (2020).
14. M. Walker, A.J.A. Harvey, A. Sen, and C.E.H. Dessent, *J. Phys. Chem. A* 117, 12590 (2013).
15. J.-D. Chai and M. Head-Gordon, *Phys. Chem. Chem. Phys.* 10, 6615 (2008).
16. Y. Zhao and D.G. Truhlar, *Theor. Chem. Acc.* 120, 215 (2008).
17. P. Winget and J.-L. Brédas, *J. Phys. Chem. C* 115, 10823 (2011).
18. M. J. Frisch, G. W. Trucks, H. B. Schlegel, G. E. Scuseria, M. A. Robb, J. R. Cheeseman, G. Scalmani, V. Barone, G. A. Petersson, H. Nakatsuji, X. Li, M. Caricato, A. V. Marenich, J. Bloino, B. G. Janesko, R. Gomperts, B. Mennucci, H. P. Hratchian, J. V. Ortiz, A. F. Izmaylov, J. L. Sonnenberg, Williams, F. Ding, F. Lipparini, F. Egidi, J. Goings, B. Peng, A. Petrone, T. Henderson, D. Ranasinghe, V. G. Zakrzewski, J. Gao, N. Rega, G. Zheng, W. Liang, M. Hada, M. Ehara, K. Toyota, R. Fukuda, J. Hasegawa, M. Ishida, T. Nakajima, Y. Honda, O. Kitao, H. Nakai, T. Vreven, K. Throssell, J. A. Montgomery Jr., J. E. Peralta, F. Ogliaro, M. J. Bearpark, J. J. Heyd, E. N. Brothers, K. N. Kudin, V. N. Staroverov, T. A. Keith, R. Kobayashi, J. Normand, K. Raghavachari, A. P. Rendell, J. C. Burant, S. S. Iyengar, J. Tomasi, M. Cossi, J. M. Millam, M. Klene, C. Adamo, R. Cammi, J. W. Ochterski, R. L. Martin, K. Morokuma, O. Farkas, J. B. Foresman, and D. J. Fox, *Gaussian 16 Rev. C.01* (Wallingford, CT, 2016).
19. K. Do, M.K. Ravva, T. Wang, and J.-L. Brédas, *Chem. Mater.* 29, 346 (2016).
20. H. Oberhofer, K. Reuter, and J. Blumberger, *Chem. Rev.* 117, 10319 (2017).
21. M. Planells, M. Nikolka, M. Hurhangee, P.S. Tuladhar, A.J.P. White, J.R. Durrant, H. Sirringhaus, and I. McCulloch, *J Mater Chem C* 2, 8789 (2014).
22. S.Y. Hong, M. Kertesz, Y.S. Lee, and O.K. Kim, *Macromolecules* 25, 5424 (1992).
23. J.L. Bredas and G.B. Street, *Acc. Chem. Res.* 18, 309 (1985).
24. S. Ghosh, V. Gueskine, M. Berggren, and I.V. Zozoulenko, *J. Phys. Chem. C* 123, 15467 (2019).
25. D. Fazzi, S. Fabiano, T.-P. Ruoko, K. Meerholz, and F. Negri, *J. Mater. Chem. C* 7, 12876 (2019).
26. G. Sini, J.S. Sears, and J.-L. Brédas, *J. Chem. Theory Comput.* 7, 602 (2011).